

Epitaxial Graphene Devices for Scanning Probe Measurements

Andrea Iagallo

NEST, Istituto Nanoscienze–CNR and Scuola Normale Superiore

Shinichi Tanabe

NTT Basic Research Laboratories, NTT Corporation

Stefano Roddaro

NEST, Istituto Nanoscienze–CNR and Scuola Normale Superiore

Makoto Takamura

NTT Basic Research Laboratories, NTT Corporation

Yoshiaki Sekine

NTT Basic Research Laboratories, NTT Corporation

Hiroki Hibino

NTT Basic Research Laboratories, NTT Corporation

Vaidotas Miseikis

Center for Nanotechnology Innovation @ NEST, Istituto Italiano di Tecnologia

Camilla Coletti

Center for Nanotechnology Innovation @ NEST, Istituto Italiano di Tecnologia

Vincenzo Piazza

Center for Nanotechnology Innovation @ NEST, Istituto Italiano di Tecnologia

Fabio Beltram

NEST, Istituto Nanoscienze–CNR and Scuola Normale Superiore

Stefan Heun

NEST, Istituto Nanoscienze–CNR and Scuola Normale Superiore



Funding

Outline

Introduction

- Dissipationless current
- Graphene on SiC

Goal

- Scanning Gate Microscopy

Mono- and bilayer composite devices in the Quantum Hall regime

- Device configuration
- Raman map & atomic force microscopy image
- Transport measurements
- Conductance calculation

Summary

Introduction

Dissipationless current

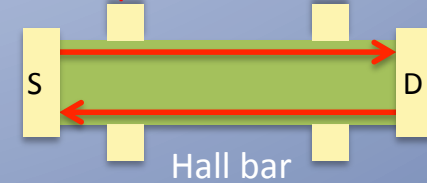
Edge current flows in quantum Hall regime

Controlling dissipationless current



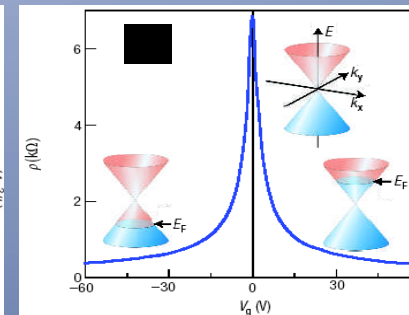
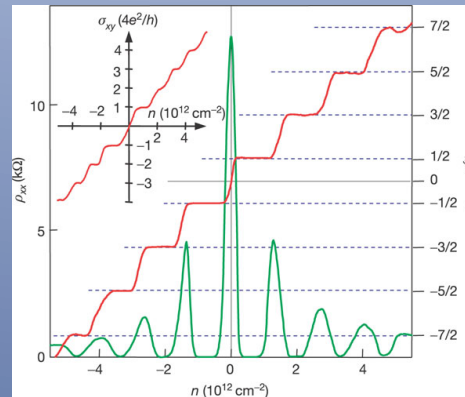
future low-energy
consumption devices

Dissipationless Current



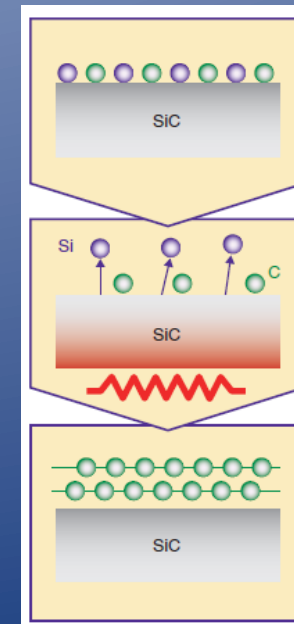
Why graphene?

- Clear quantum Hall effect is observed
- High mobility
- Filling factor differs between mono- and bilayer graphenes



Graphene on SiC

Epitaxial growth by Si sublimation technique
large area, high quality, insulating substrate



A. K. Geim and K. S. Novoselov, Nature Mater. 6, 183 (2007)

K. S. Novoselov et al., Nature 438, 197 (2005)

Y. Zhang et al., Nature 438, 201 (2005)

Hiroki Hibino et al., NTT Technical Review 8,(2010)

Goal: Scanning Gate Microscopy

A voltage-biased AFM tip is scanned above a sample surface. This creates a perturbation below the tip, which locally modifies the potential landscape of a device (typically 2DEGs, graphene, nanowires).

Scanning Gate Microscopy: low-T, high-B AFM
Topographic imaging + movable electrostatic gate

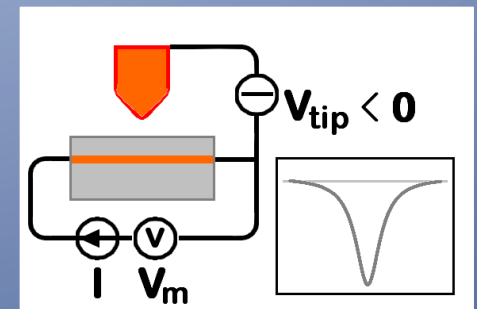
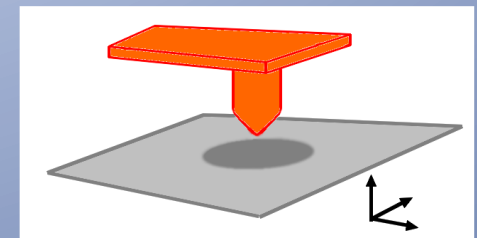
→ 2D imaging of transport properties

Space information: $G(x,y)$

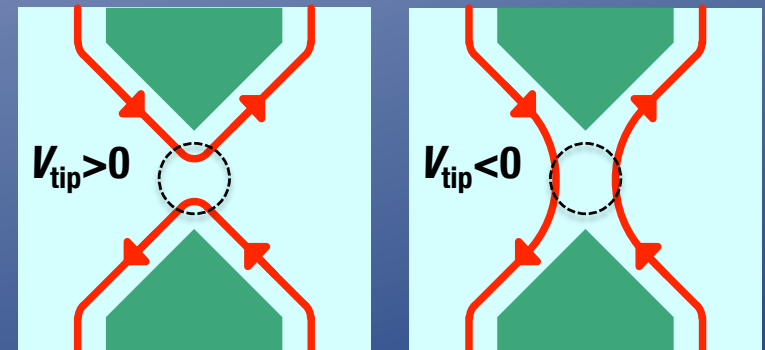
Extension / space distribution of electronic states
Relevant length scales (inter-channel relaxation length)
Size-dependent effects (edge state mixing)

...

resolution	≤ 10 nm
stability	months
temperature	300 mK
Magnetic field	0-9 T



Side-gate structure



Tip voltage is applied at the center

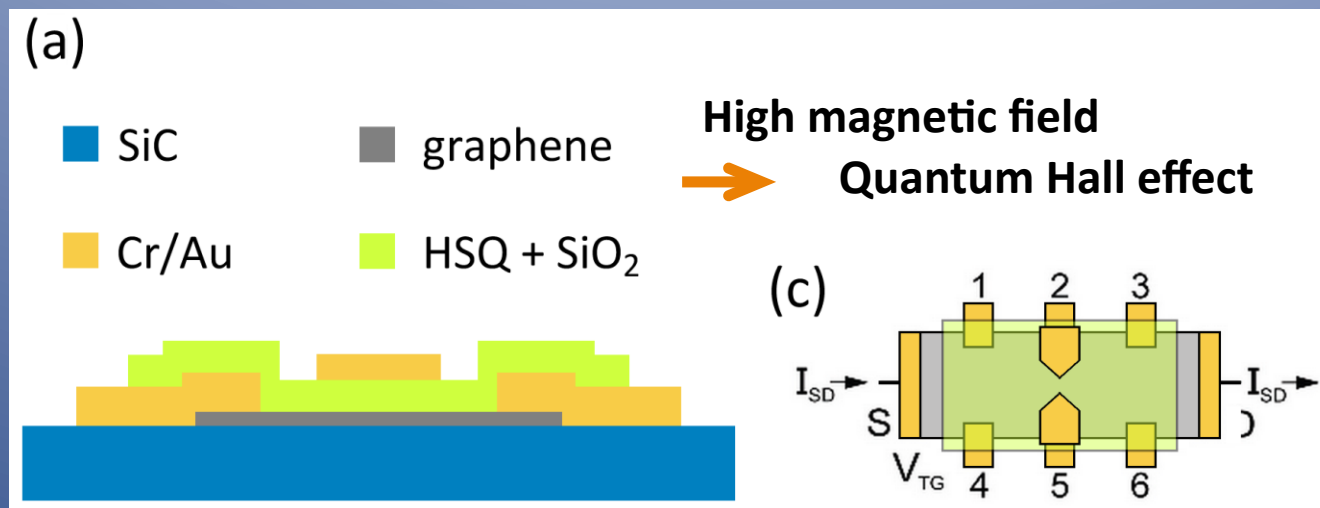
M. A. Topinka et al., Nature 410 (2001).

R. Crook et al., Science, 312 (2006).

N. Paradiso et al., Phys. Rev. Lett., 108 (2012).

Fabrication: Side-Gated Devices

- Epitaxial graphene grown on the Si face of SiC (0001).
- Large area Hall bars (300 μm x 50 μm)
- Gate insulator: HSQ (Hydrogen Silsequioxane) (140 nm) + SiO₂ (40 nm)
- Electrode: Cr/Au (10/180 nm)

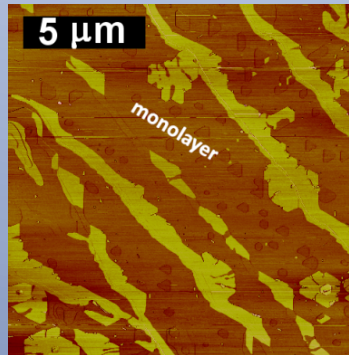
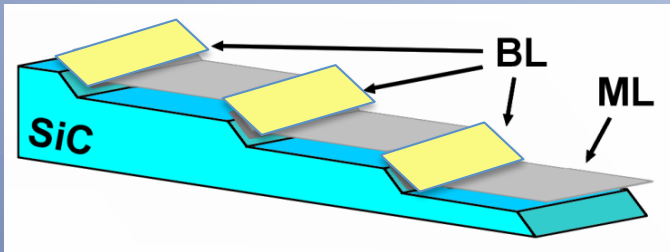
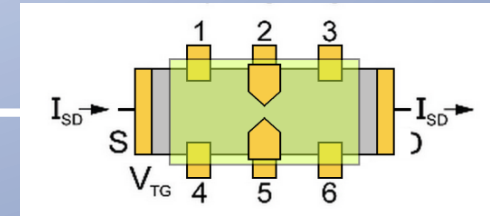


S. Tanabe, Y. Sekine, H. Kageshima, M. Nagase, and H. Hibino, Phys. Rev. B 84, 115458 (2011).

First Step

Characterization of the electric properties of the device **without applying the side-gate voltage and AFM tip voltage**

Sample: AFM & Raman



~ few μm wide monolayer regions on SiC terraces

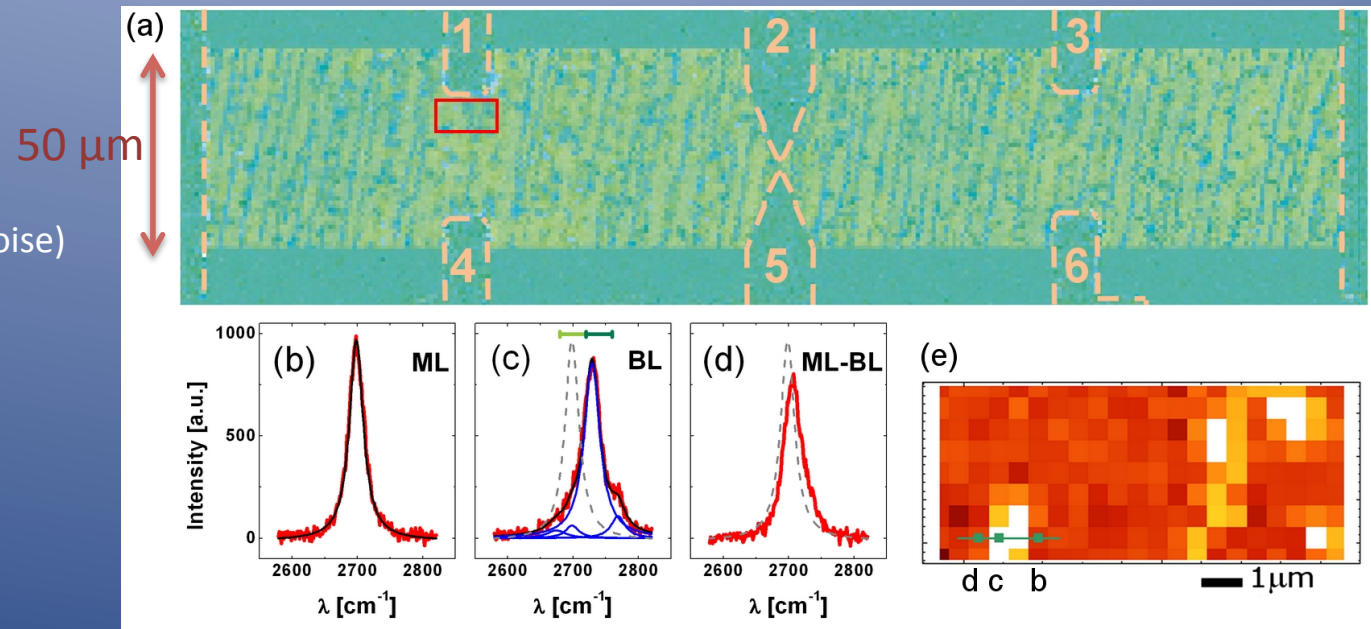
$\leq 1 \mu\text{m}$ wide bilayer domains along step edges

Raman spectra @ Room Temperature

(Renishaw Micro-Raman)
514 nm laser excitation
spot diameter $< 1 \mu\text{m}$.
step-size of $0.5 \mu\text{m}$
integration times up to 10 s (low noise)

Monolayer: single Lorentzian
 $\rightarrow 2680\text{-}2720 \text{ cm}^{-1}$

Bilayer: 4 Lorentzians
 $\rightarrow 2720\text{-}2760 \text{ cm}^{-1}$



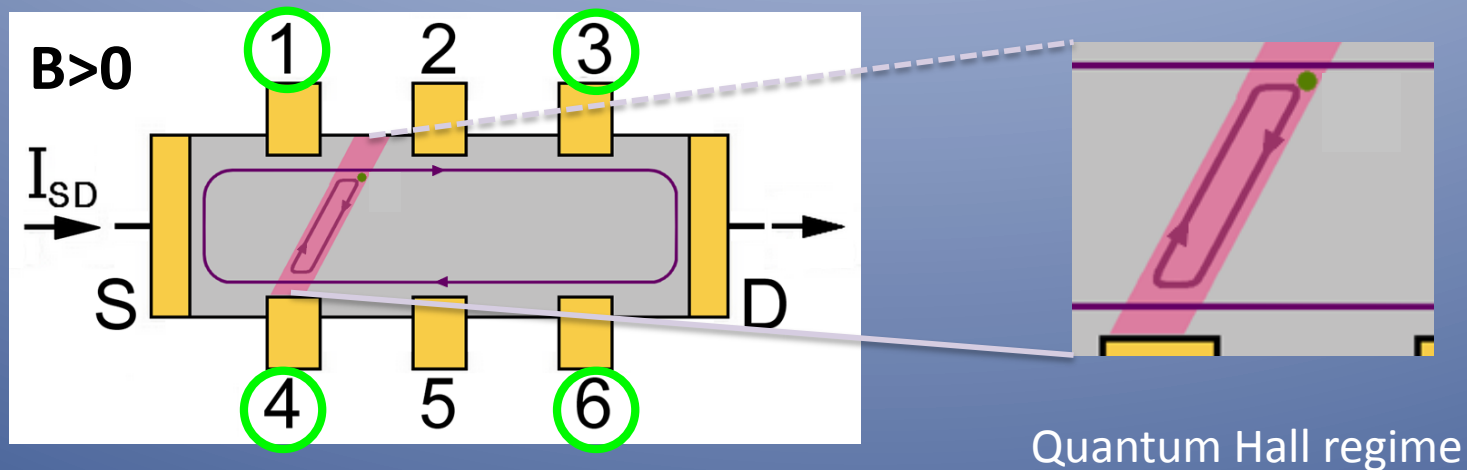
The Hall bar is intersected by tens of SiC step edges, onto which elongated bilayer domains are present.

\rightarrow Bilayer stripe connect one side of the device to the other

Configuration of mono- and bilayers

From the experimental results of magnetoresistance

Bilayer stripe (red) crossing Hall bar

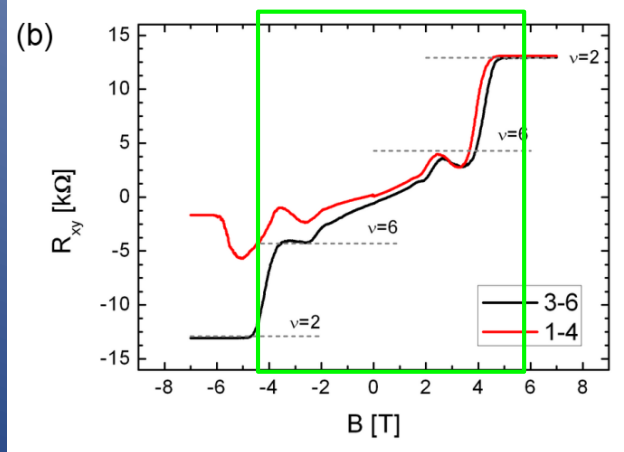
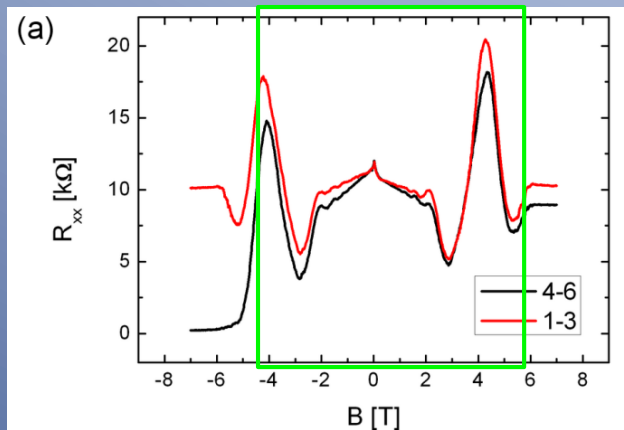


longitudinal resistance R_{xx} : R_{1-3}, R_{4-6}

transverse resistance R_{xy} : R_{1-4}, R_{3-6}

Magnetoresistance (1): Low Magnetic Field

@ 250 mK



$|B| < 5 \text{ T}$ Conventional quantum Hall effect of monolayer graphene

longitudinal resistance R_{xx} :

similar at both device sides;

typical behavior expected for clean monolayer:

weak localization around $B=0$;

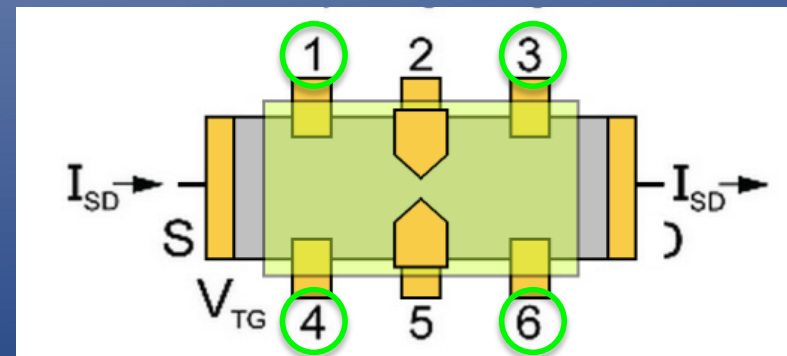
magneto-oscillations (precursory to the Shubnikov-de Haas).

transverse resistance R_{xy} :

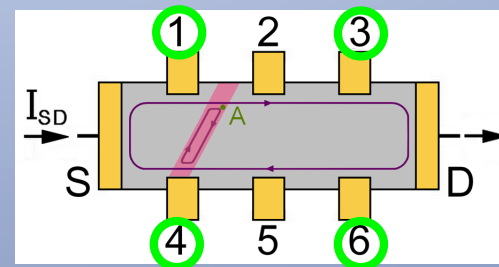
similar for both contact pairs;

monotonous dependence;

$\nu=6$ plateau.

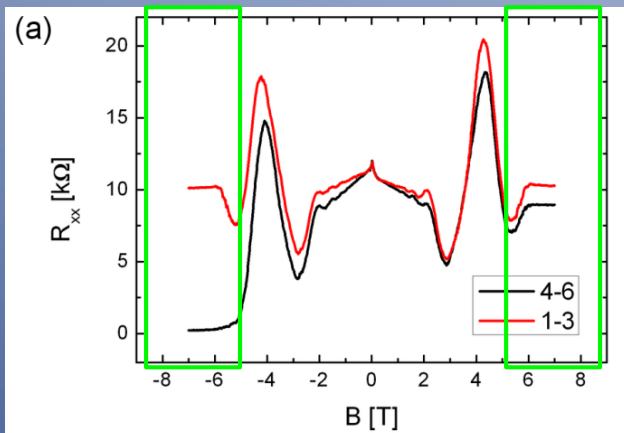


Magnetoresistance (2): High Magnetic Field



Bilayer stripe (red)
crossing Hall bar

@ 250 mK

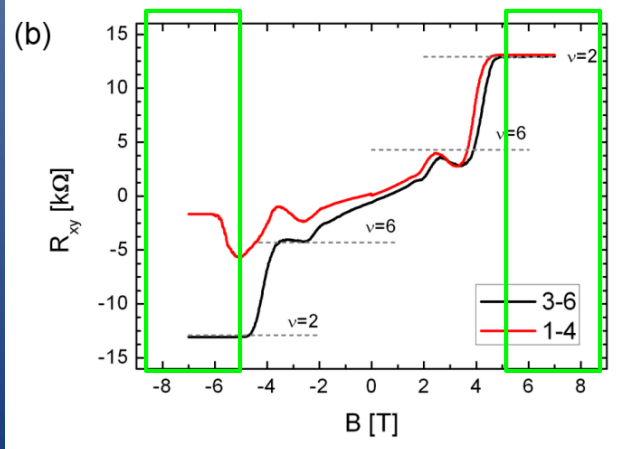


$|B| > 5 \text{ T}$ Anomalous Quantum Hall effect

longitudinal resistance R_{xx} :

1-3 : invariant to inversion of B ; $R \approx 10 \text{ k}\Omega$

4-6 : asymmetric upon inversion of B ; SdH for $B < 0$ only



transverse resistance R_{xy} :

3-6 : conventional (symmetric) half-integer QHE; $\nu = \pm 2$ plateaus

1-4 : asymmetric upon inversion of B ; $R_{1-4} = -1.6 \text{ k}\Omega$ for $B < 0$

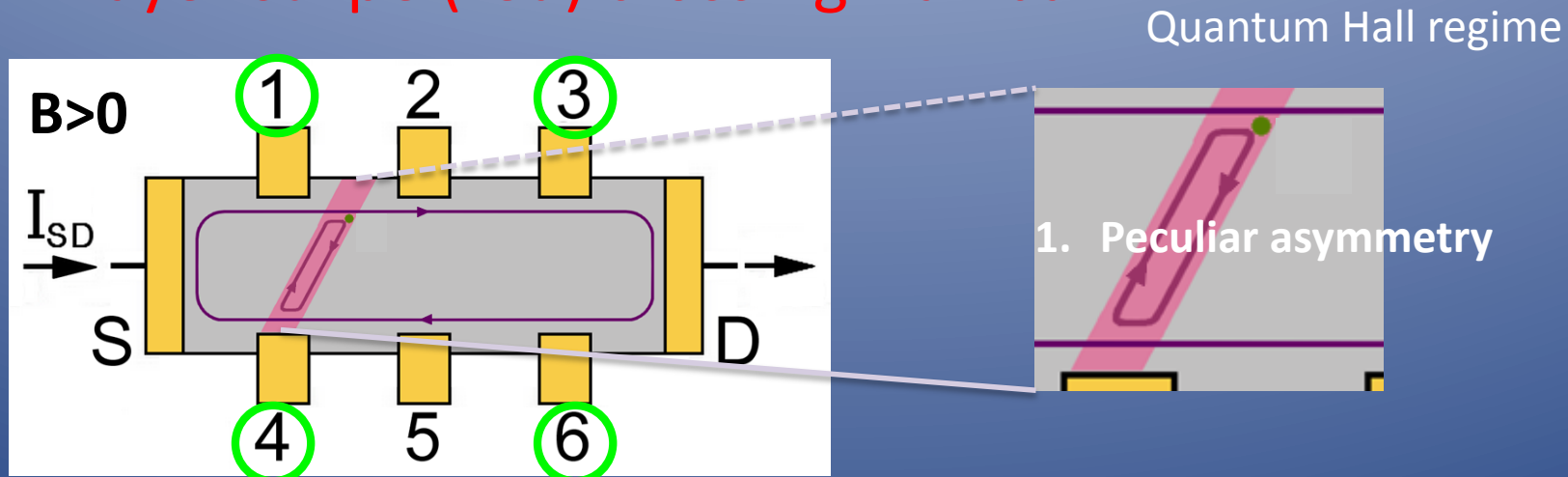


1. B-dependent effect
2. Flat resistance values
3. Peculiar asymmetry

Configuration of mono- and bilayers

- | | | | | |
|---------------------------|---|---------------------------------|---|---|
| 1. Effect dependent on B | → | 1. Quantum Hall Effect | → | Quantum Hall effect |
| 2. Flat resistance values | → | 2. Anomalous quantized plateaus | → | Involving edge channels in bilayer |
| 3. Peculiar asymmetry | → | 3. Chirality of edge states | → | Only one possible configuration |

Bilayer stripe (red) crossing Hall bar



Filling factor

Monolayer graphene

$$\nu_M = \pm 2(2n+1) = \pm 2, \pm 6, \pm 10, \dots$$

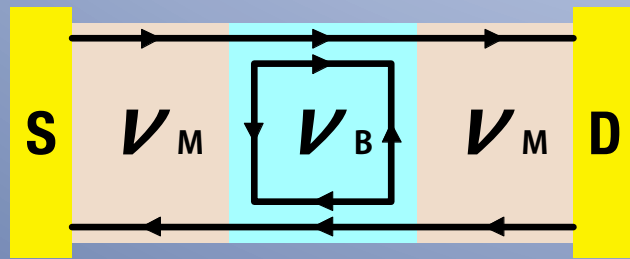
$$n = 0, 1, 2, \dots$$

Bilayer graphene

$$\nu_B = \pm 4n = \pm 4, \pm 8, \pm 12, \dots$$

$$n = 1, 2, 3, \dots$$

Landauer-Büttiker approach



$$|\nu_B| > |\nu_M|, \nu_B \cdot \nu_M > 0$$

- Mixing of channel
- Current conservation at boundary between mono- and bilayer graphene

$$I_i = e/h [(\nu - r_{ii})\mu_i + \sum T_{ij} \mu_j]$$

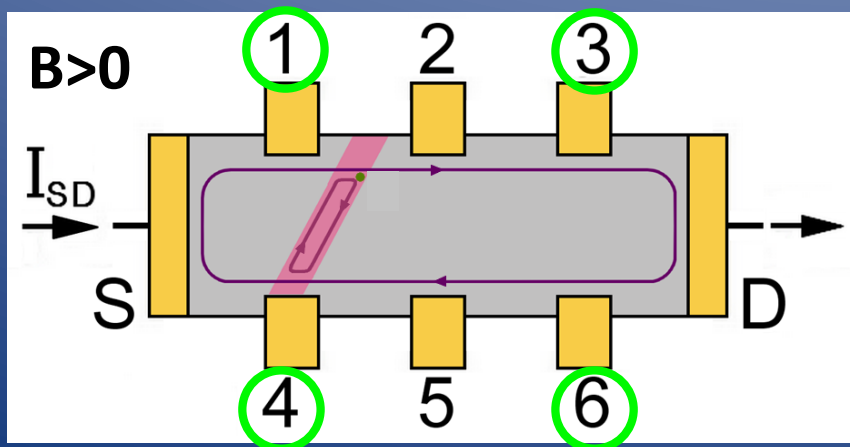
$$I_S = I, I_D = -I, I_i = 0$$

I_i : current

r_{ii} : total reflection coefficient at electrode i
($r_{ii} = 0$ for ideal lead)

μ_i : electrochemical potential

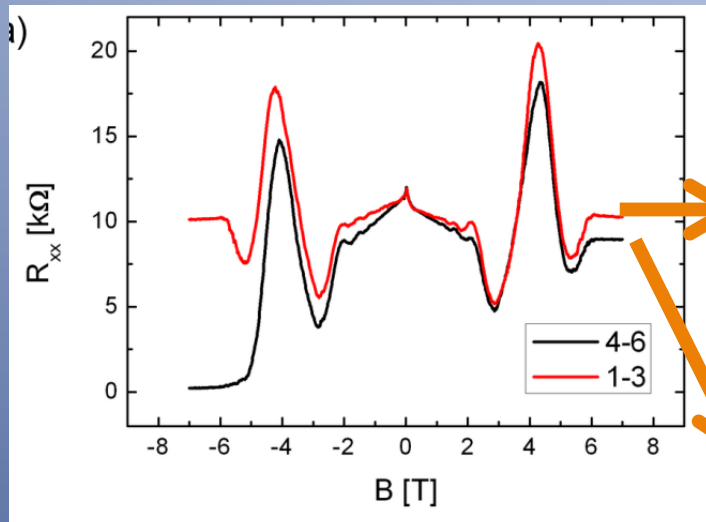
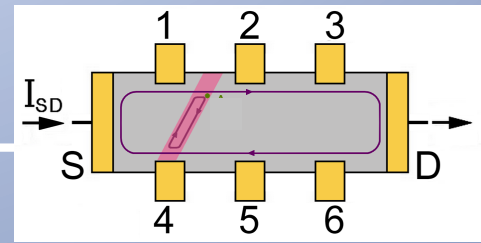
T_{ij} : total transmission coefficient from i to j electrodes
(probability ejected into ν proportional to $1/\nu$ for each electron)



	R_{1-3}	R_{4-6}	R_{1-4}	R_{3-6}
$B > 0$ (CW)	$\frac{\nu_B - \nu_M}{\nu_B \nu_M}$	$\frac{\nu_B - \nu_M}{\nu_B \nu_M}$	$\frac{1}{\nu_M}$	$\frac{1}{\nu_M}$
$B < 0$ (CCW)	$\frac{\nu_B - \nu_M}{\nu_B \nu_M}$	0	$-\frac{1}{\nu_B}$	$-\frac{1}{\nu_M}$

in a unit of h/e^2

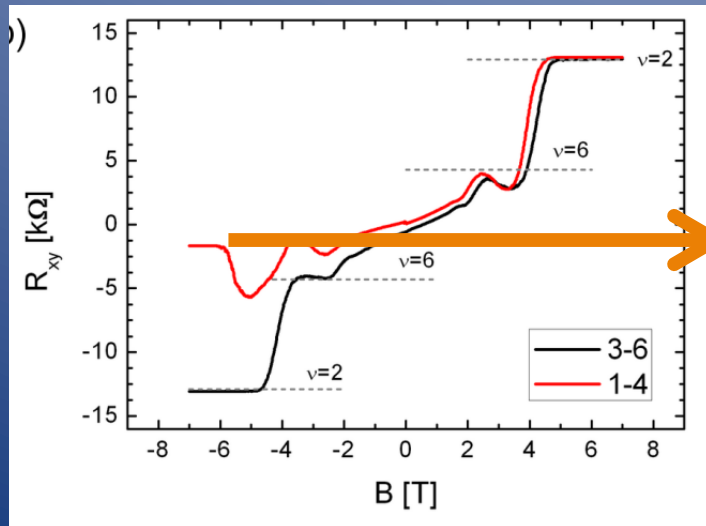
Quantitative approach



$$R_{1-3} = \frac{\nu_B - \nu_M}{\nu_B \nu_M} = 0.393 \times \frac{h}{e^2}, \quad \nu_M = 2$$

$$\nu_B = 9.3 \approx 8$$

$$\text{uncertainty } \Delta R_{XX} = 0.051 \times \frac{h}{e^2} \approx 1.3 \text{ k}\Omega$$



$$R_{1-4} = -\frac{1}{\nu_B} = -0.064 \times \frac{h}{e^2} \approx 1.65 \text{ k}\Omega$$

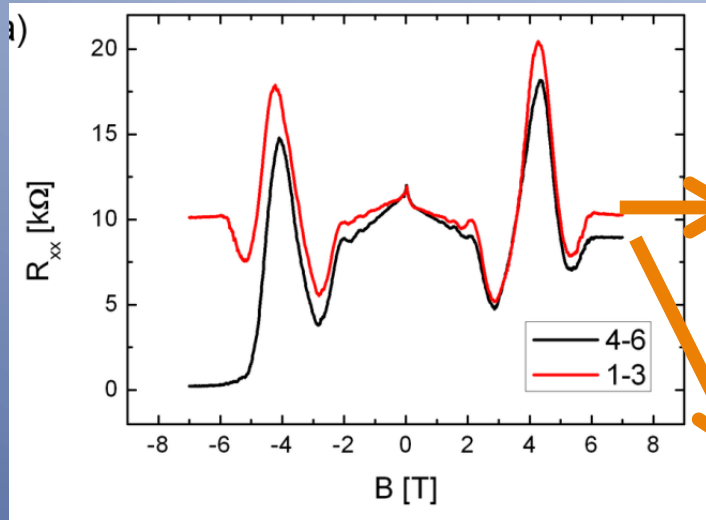
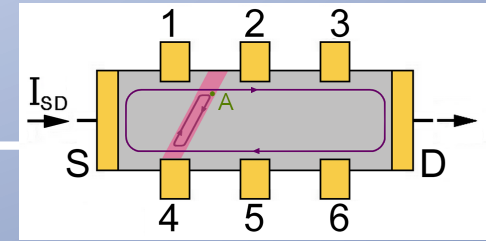
$$\text{Using } \nu_B = 8 \rightarrow R_{1-4} = -0.125 \times \frac{h}{e^2} \approx 3.23 \text{ k}\Omega$$

Summary

Hall bar oriented perpendicularly to the SiC(0001) step edges:

- We observe an **asymmetric B-dependence** of the magnetoresistance due to the continuous **bilayer stripe** crossing the device.
- We propose a **quantitative model** involving the simultaneous coexistence of quantum Hall conditions in the monolayer and bilayer regions, at **different filling factors**, which fully account for the asymmetry and the observed quantized resistance values.
- The transport channels in the bilayer are responsible for **mixing of the edge channels** in the monolayer and deviations from the conventional quantum Hall effect.

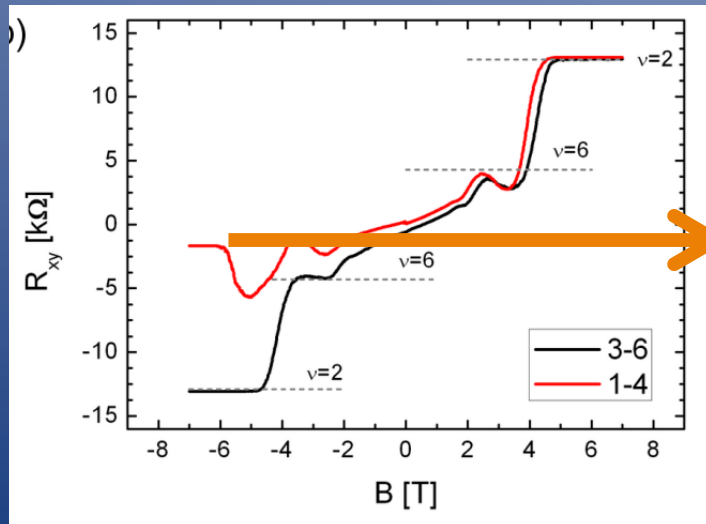
Quantitative approach



$$R_{1-3} = \frac{\nu_B - \nu_M}{\nu_B \nu_M} = 0.393 \times \frac{h}{e^2}, \quad \nu_M = 2$$

$$\nu_B = 9.3 \approx 8$$

$$\text{uncertainty } \Delta R_{XX} = 0.051 \times \frac{h}{e^2}$$



$$R_{1-4} = -\frac{1}{\nu_B} = -0.064 \times \frac{h}{e^2}$$

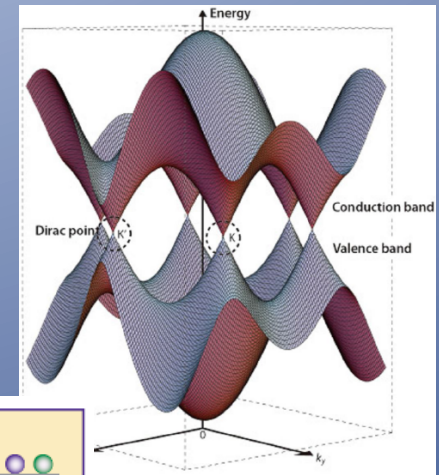
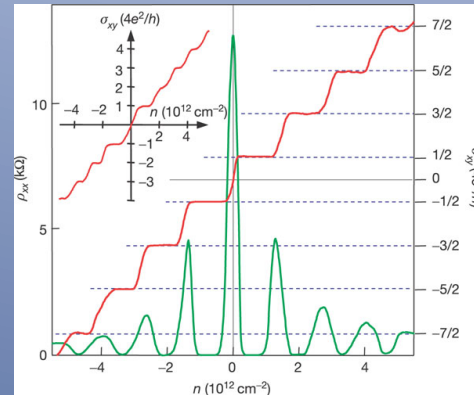
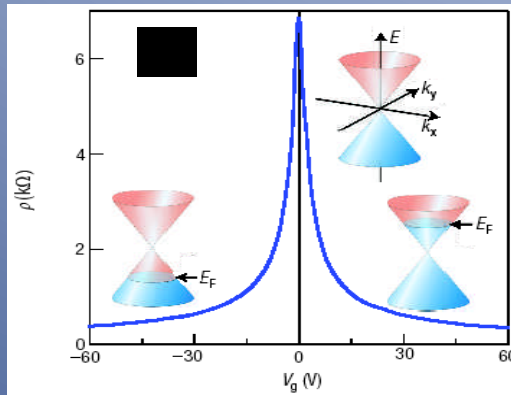
$$\text{Using } \nu_B = 8 \rightarrow R_{1-4} = -0.125 \times \frac{h}{e^2}$$

Motivation: Graphene

Why graphene?

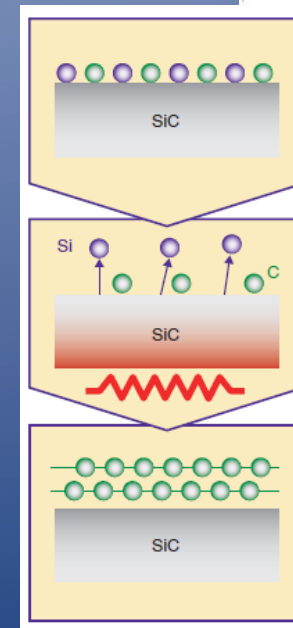
Unique Electronic Properties: Relativistic carriers, Klein tunneling, snake states...

Unique Conformational Properties: Single atom layer, exposed surface



Ways to make graphene

- exfoliation from graphite (small)
- chemical vapor deposition (large, conductive substrate)
- epitaxial growth on SiC (large, wide-gap substrate) ←



A. K. Geim and K. S. Novoselov, Nature Mater. 6, 183 (2007)

K. S. Novoselov et al., Nature 438, 197 (2005)

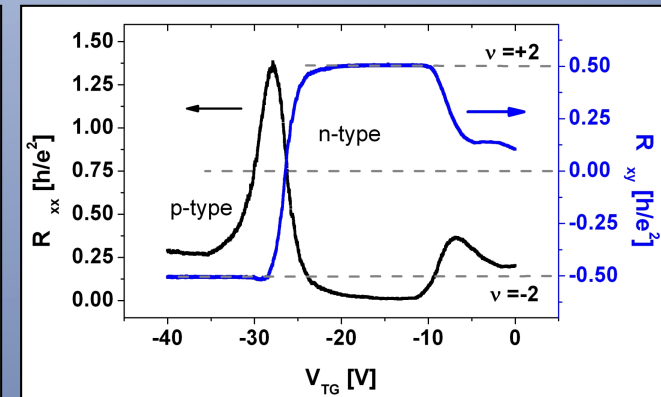
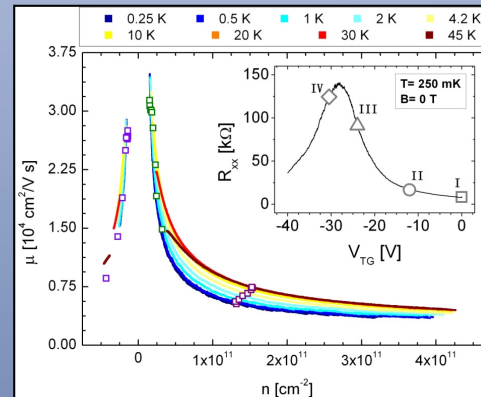
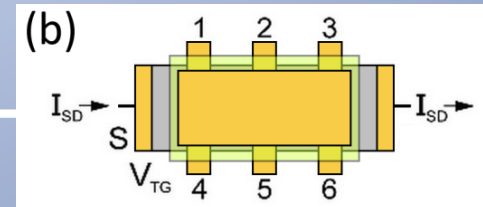
Y. Zhang et al., Nature 438, 201 (2005)

Hiroki Hibino et al., NTT Technical Review 8,(2010)

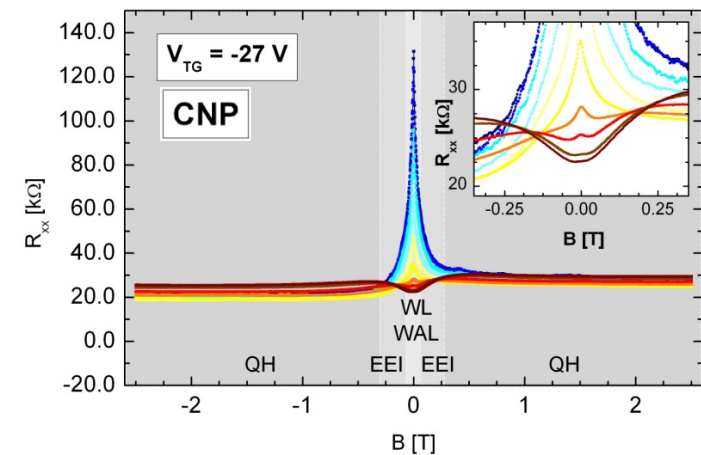
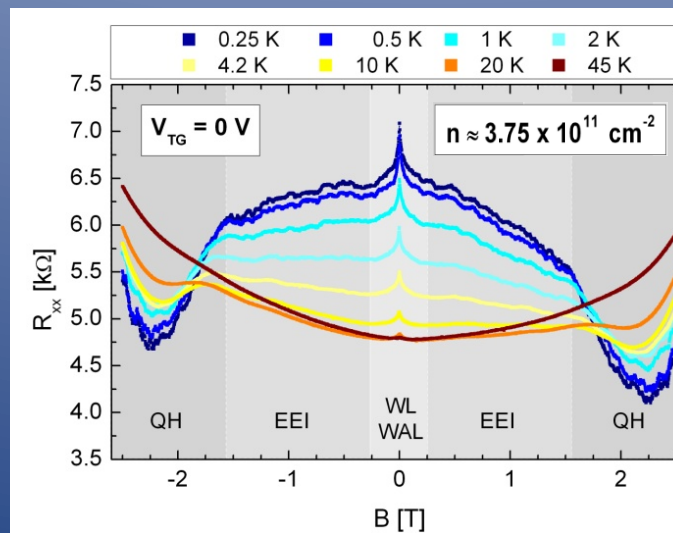
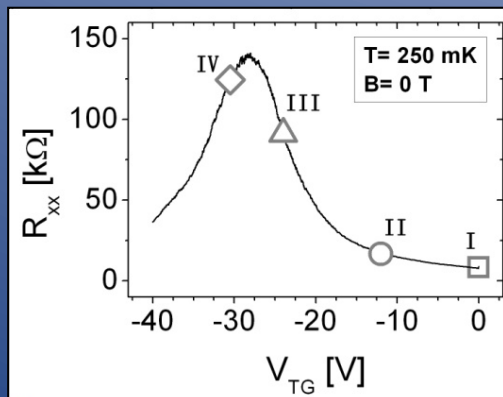
Device for low magnetic field

Tunable carrier density (and mobility)
 $n = -2 \times 10^{10}$ to 4×10^{11} cm^{-2}
 $\mu = 0 - 35000$ cm^2/Vs

Monolayer graphene
 (i.e., half-integer quantum Hall effect)

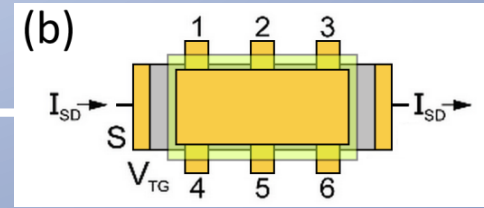


Dominant effect depends on carrier density



A. Iagallo, S. Tanabe, S. Roddaro, M. Takamura, H. Hibino, and S. Heun, Phys. Rev. B 88, 235406 (2013)

Electron-Electron interaction/01



$$\frac{\Delta R_{xx}}{R_0^2} \approx \underbrace{\left[(\omega_c \tau_0)^2 - 1 \right]}_{\text{Quadratic magnetoresistance}} \frac{e^2}{2\pi^2 \hbar} \underbrace{\left[K_{ee} \ln \left(\frac{k_B T \tau_0}{\hbar} \right) \right]}_{\text{Fermi liquid}}$$

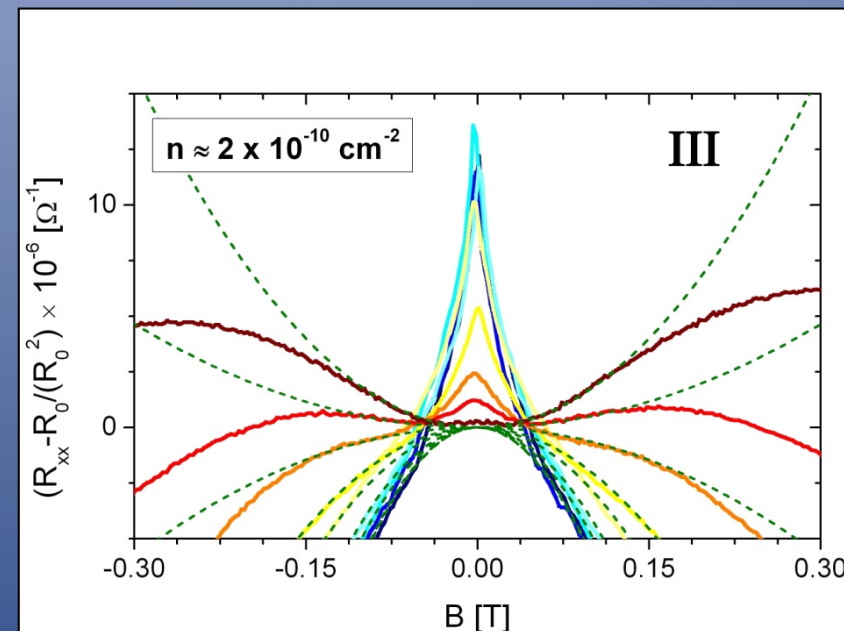
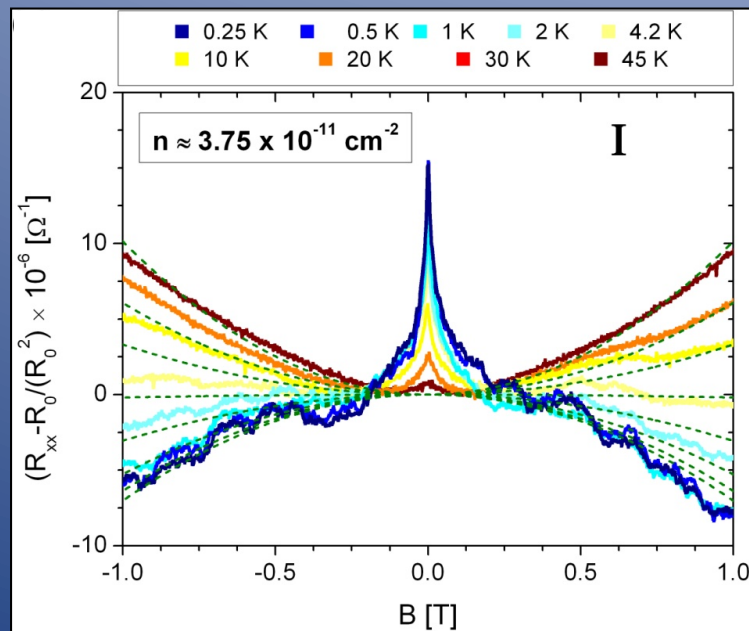
$$\omega_c = \left(v_F e / \hbar \sqrt{\pi n} \right) B$$

Quadratic
magnetoresistance

$$A = K_{ee} \ln(k_B T \tau_0 / \hbar) \text{ (curvature)}$$

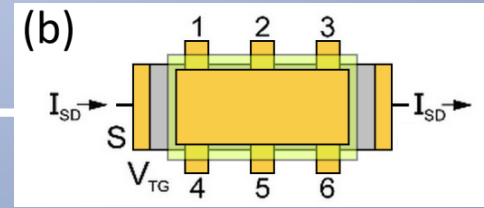
K_{ee} : (adimensional) strength of interaction
 $\sim \ln(T)$ (Fermi liquid)

A. A. Kozikov et al., Phys. Rev. B 82, 075424 (2010).
J. Jobst et al., Phys. Rev. Lett. 108, 106601 (2012).
S. Lara-Avila et al., Phys. Rev. Lett. 107, 166602 (2011)



A. Iagallo, S. Tanabe, S. Roddaro, M. Takamura, H. Hibino, and S. Heun, Phys. Rev. B 88, 235406 (2013)

Electron-Electron interaction/02



$$\frac{\Delta R_{xx}}{R_0^2} \approx \underbrace{\left[(\omega_c \tau_0)^2 - 1 \right]}_{\omega_c} \frac{e^2}{2\pi^2 \hbar} \underbrace{\left[K_{ee} \ln \left(\frac{k_B T \tau_0}{\hbar} \right) \right]}_A$$

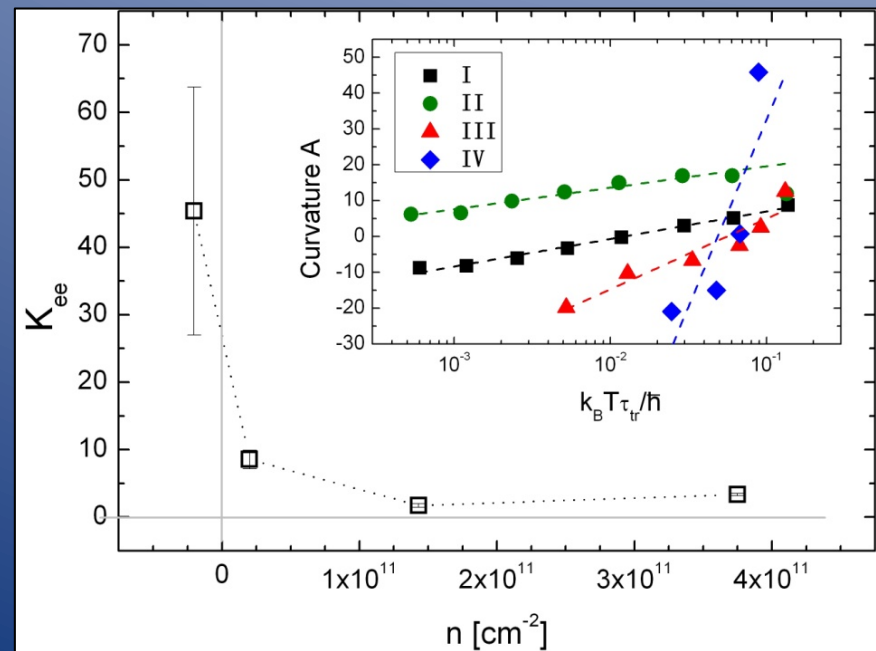
$$\omega_c = \left(v_F e / \hbar \sqrt{\pi n} \right) B$$

Quadratic magnetoresistance

$$A = K_{ee} \ln(k_B T \tau_0 / \hbar) \text{ (curvature)}$$

K_{ee} : (adimensional) strength of interaction
 $\sim \ln(T)$ (Fermi liquid)

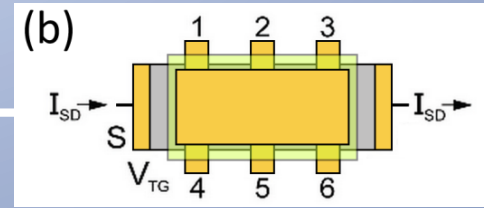
A. A. Kozikov et al., Phys. Rev. B 82, 075424 (2010).
 J. Jobst et al., Phys. Rev. Lett. 108, 106601 (2012).
 S. Lara-Avila et al., Phys. Rev. Lett. 107, 166602 (2011)



1. Linear slope \rightarrow Electrons in disordered graphene behaves as a Fermi liquid.
2. Clear n-dependence of K_{ee} at low density, not accounted for by present theory (dielectric environment? charge inhomogeneity around CNP?)

A. Iagallo, S. Tanabe, S. Roddaro, M. Takamura, H. Hibino, and S. Heun, Phys. Rev. B 88, 235406 (2013)

Quantum Interference/01



After subtracting EEI contribution

$$\frac{\Delta R_{xx}}{R_0^2} = -\frac{e^2}{\pi h} \left[F\left(\frac{\tau_B^{-1}}{\tau_\varphi^{-1}}\right) - F\left(\frac{\tau_B^{-1}}{\tau_\varphi^{-1} + 2\tau_{iv}^{-1}}\right) - 2F\left(\frac{\tau_B^{-1}}{\tau_\varphi^{-1} + \tau_*^{-1}}\right) \right]$$

E. McCann et al., Phys. Rev. Lett. 97, 146805 (2006)

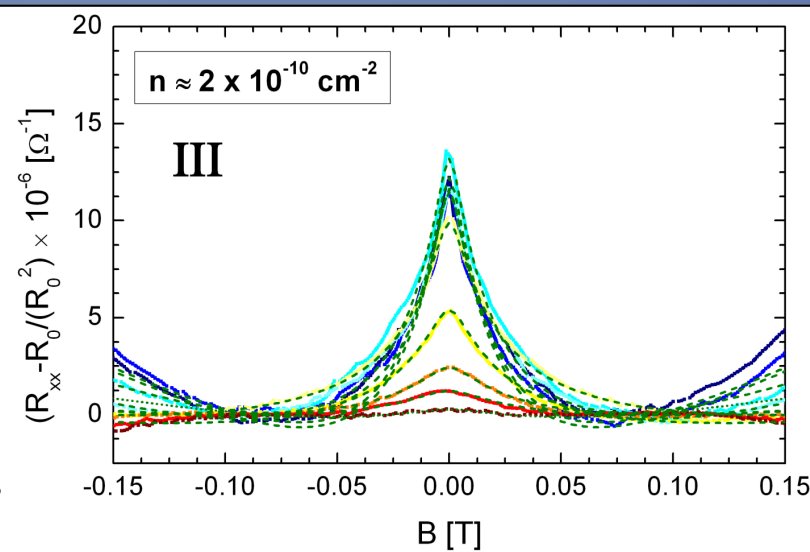
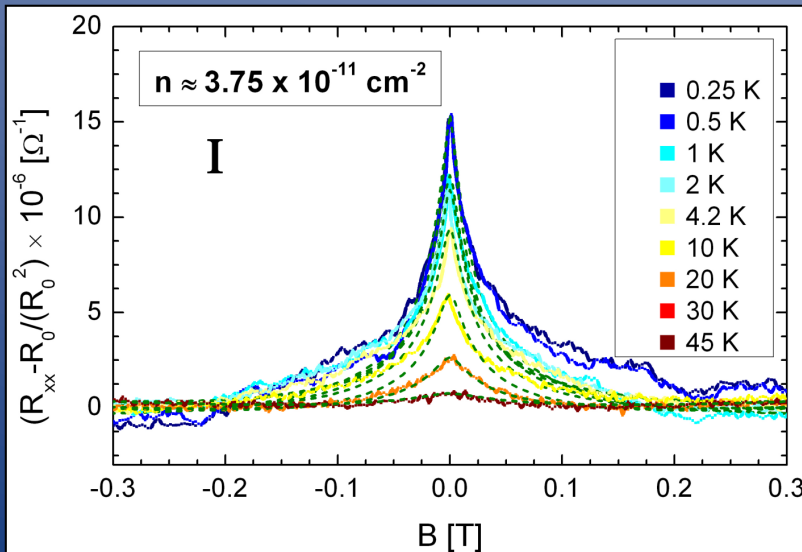
$F(z) = \ln(z) + \psi(0.5 + z^{-1})$, $\psi(x)$ is the digamma function

τ_φ = dephasing time

τ_{iv} = inter - valley scattering

τ_* = intra - valley scattering

$$\tau_B^{-1} = \frac{4DeB}{\hbar}, D = \text{diffusion coefficient}$$



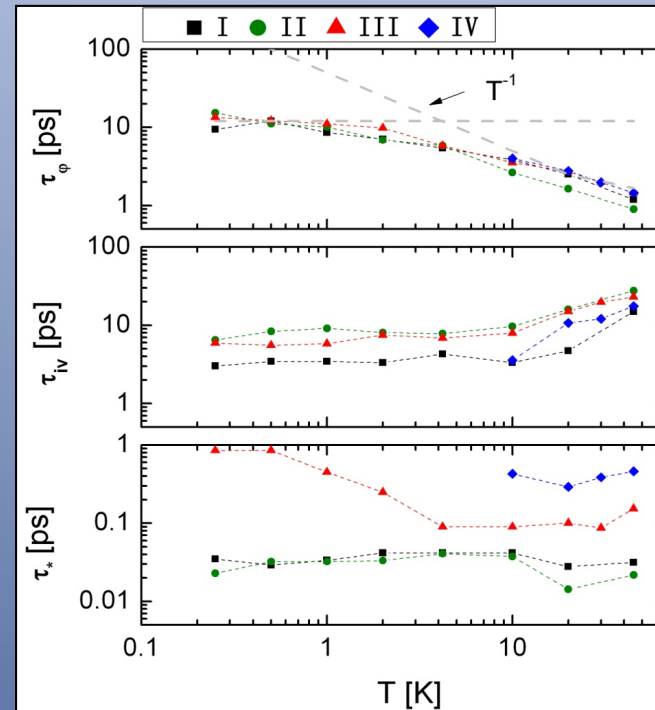
A. Iagallo, S. Tanabe, S. Roddaro, M. Takamura, H. Hibino, and S. Heun, Phys. Rev. B 88, 235406 (2013)

Quantum Interference/02

Dephasing time τ_φ :
Saturation in T ;
Constant in n .

Intervalley scattering
time τ_{iv} :
Almost constant in T ;
Small variation with n .

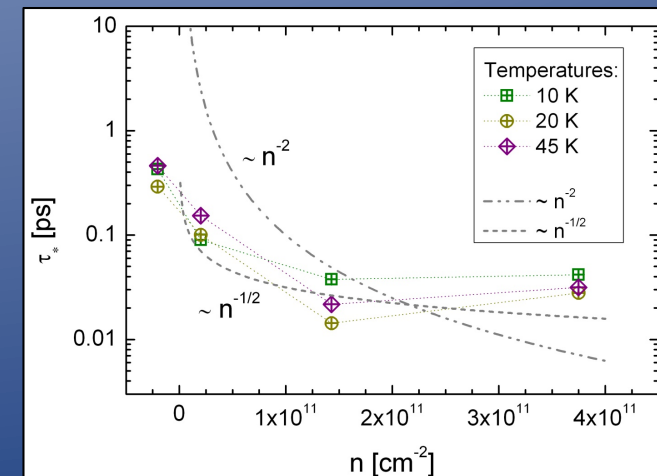
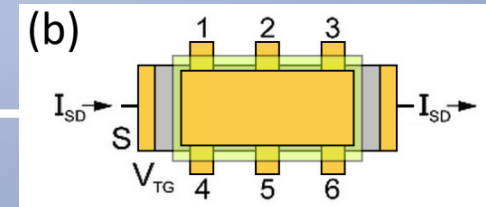
Intravalley scattering
time τ_* :
Small variation in T ;
Large variation with n .



τ_* : unexpected density dependence

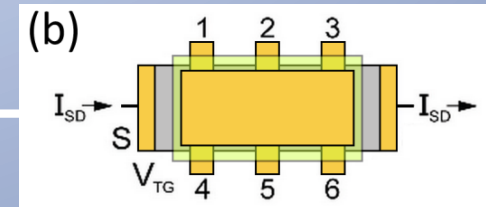
trigonal warping gives $\sim n^{-2}$

The observed dependence is larger
than the sole trigonal warping



A. Iqbal, S. Tanabe, S. Roddaro, M. Takamura, H. Hibino, and S. Heun, Phys. Rev. B 88, 235406 (2013)

Low magnetic field summary



- We presented a **systematic** analysis of magnetotransport properties in epitaxial graphene grown on the Si-terminated face of SiC.
- We describe **EI** in graphene with the current theory for disordered systems, and we find an unexpected dependence of the interaction parameter K_{ee} on carrier density.
- Fitting the **quantum interference** correction, we find that the dephasing and intervalley times are almost constant, while the intravalley scattering time shows a peculiar dependence on density, different from the sole warping term.
- Our results stress the **role of charge density** in determining quantum interference and EI, and the necessity of further investigation of its impact **on the low-field magnetoresistance** of graphene devices.

A. Iagallo, S. Tanabe, S. Roddaro, M. Takamura, H. Hibino, and S. Heun, Phys. Rev. B 88, 235406 (2013)

Thank you for your attention

Funding:



Yoshiaki Sekine
Andrea Iagallo
Shinichi Tanabe
Stefano Roddaro
Makoto Takamura
Hiroki Hibino
Vaidotas Miseikis
Camilla Coletti
Vincenzo Piazza
Fabio Beltram
Stefan Heun